Supplementary Information

Linking sea level rise and socioeconomic indicators under the Shared Socioeconomic Pathways

Alexander Nauels[1*], *Joeri Rogelj*[2,3,4], *Carl-Friedrich Schleussner*[5,6], *Malte Meinshausen*[1,6], *Matthias Mengel*[6]

(1) Australian-German Climate & Energy College, University of Melbourne, Melbourne, Australia

(2) Energy Program, International Institute for Applied Systems Analysis, Laxenburg, Austria

(3) Institute for Atmospheric and Climate Science, ETH Zurich, Zurich, Switzerland

(4) Environmental Change Institute, University of Oxford, Oxford, UK

(5) Climate Analytics, Berlin, Germany

(6) Potsdam Institute for Climate Impact Research, Potsdam, Germany

(*) email alexander.nauels@climate-energy-college.org

Calibration of the Antarctic solid ice discharge contribution

In order to emulate the future Antarctic Ice Sheet (AIS) sea level response presented in DeConto and Pollard [2016], we replace the AIS Solid Ice Discharge (SID) component from Nauels et al. [2017] with a new parameterization that is able to capture the suggested additional processes of hydrofracturing and ice cliff failure.

We use the 29-member DeConto and Pollard [2016] time series of Antarctic sea level contributions as the reference dataset for our calibration. The DeConto and Pollard [2016] (DP16) projections are provided until 2500. The ensemble was forced with bias-adjusted ocean temperatures in the Bellingshausen and Amundsen Seas and assumes a Pliocene sea level sensitivity of 5-15 m relative to year 2000 levels. We use annual global mean surface air temperature output from the CCSM4 model, which mimics the original forcing setup from DeConto and Pollard [2016], to drive our revised AIS SID parameterization. For RCP8.5, the CO_2 equivalent forcings are held constant beyond 2175 at eight times above pre-industrial values. Post 2300, ocean temperatures are maintained at 2300 levels until 2500 in MAGICC. The fixed post-2300 ocean only influences our global-mean-temperature-driven parametrization through the atmosphere-ocean interaction within MAGICC. This effect is minor.

For every reference ensemble member, we define the overall AIS Solid Ice Discharge (SID) global sea level contribution to be:

$$AIS_t^{SID} = AIS_{max}^{SID} - AIS_{Vdis(t)}^{SID}$$

With AIS_t^{SID} defined as the difference of the initial maximum ice volume susceptible to discharge and the remaining ice volume available for discharge at time step *t*. The maximum ice volume, AIS_{max}^{SID}, is set as the maximum DP16 ice loss between 1950 and 2500 of 17.56 m. The time-dependent $AIS_{Vdis(t)}^{SID}$, the global Antarctic ice volume in sea-level equivalent, is determined as follows: For $t = 0$, $AIS_{Vdis(t)}^{SID} = AIS_{max}^{SID}$. The remaining ice volume susceptible to discharge at time step *t*, $AIS_{Vdis(t)}^{SID}$, has the following functional form:

$$AIS_{Vdis(t)}^{SID} = AIS_{Vdis(t-1)}^{SID} - \alpha * AIS_{Vdis(t-1)}^{SID} * sign(T - T_0)(T - T_0)^2 + \varphi(t)$$

with the annual discharge being the product of the discharge sensitivity α, the AIS ice volume $AIS_{Vdis(t-1)}^{SID}$ available at time step *t-1* and the quadratic sensitivity to temperature deviation, plus a fast discharge term $\varphi(t)$. The quadratic temperature sensitivity term is relative to a reference temperature T_0 at which the ice sheet would be stable on long time scales. The additional fast discharge term consists of a heavyside function times a discharge constant gamma:

$$\varphi(t) = \gamma * \theta(T(t) - T_{threshold})$$

Thus, the fast discharge term $\varphi(t)$ equals 0 if the global surface air temperature anomaly T(t) is below the threshold temperature anomaly $T_{threshold}$ at time step *t*. We here define T_0 and $T_{threshold}$ relative to 1850. As they are part of the free parameters that are calibrated, they would adjust if the reference period was changed.
We enforce that not more ice can be lost than is still available as ice volume, so

$$\frac{dAIS_{Vdis(t)}^{SID}}{dt} < AIS_{Vdis(t-1)}^{SID}$$

This condition is only relevant for the here presented numbers until 2100 through its influence on the calibration.

We calibrate α, γ, T_0, and $T_{threshold}$ for each of the 29 ensemble members of the reference data under RCP 2.6, RCP 4.5, and RCP 8.5 over the period 1950 to 2500 (see Table S1). The individual parameter calibration ranges for α (0.0 to 0.001), γ (0 to 100 mm), T_0(0.0 to 10.0 °C), and $T_{threshold}$ (0.0 to 10.0 °C) have been determined through iterative testing to ensure convergence to a global optimum. We aim to minimize the residual sum of squares (RSS) for all RCP scenarios together per ensemble member. We weigh the RSS for the individual RCP scenarios by the corresponding global mean SLR range of the reference data between 1950 and 2500 to ensure that RCP85 does not dominate the error and the calibrated parameters. For the least square optimization, we use an automated Nelder-Mead simplex routine [Nelder & Mead 1965; Lagarias et al. 1998], with a termination tolerance of $1e^{-10}$ and a maximum iteration number of 10,000.

The optimal parameter sets are listed in Table S1. We can see that the calibration produces fits that are able to capture the full ensemble of DeConto and Pollard [2016] projections rather well (Figure S1). Please note that the revised AIS discharge component is generally only used for projections out to 2100 and 2300.

Probabilistic projections following Nauels et al. [2017]

We project global sea level rise following the methodology of Nauels et al. [2017]. For every SSP scenario, we run the MAGICC sea level model with 600 historically constrained parameter sets that have been derived using a probabilistic Metropolis–Hastings Markov chain Monte Carlo method [Meinshausen et al. 2009]. This approach has been extended to also reflect carbon-cycle uncertainties [Friedlingstein et al. 2014] and the climate sensitivity range of IPCC AR5 [Rogelj et al. 2012; Flato et al. 2013; Rogelj et al. 2014]. As part of every run, we randomly draw one of the 29 optimal parameter sets of AIS discharge for each of the 600 ensemble members as we treat all 29 calibrated members AIS discharge members as equally possible. Thus, we generate 600 AIS discharge SLR projections per SSP scenario that reflect the full model range of the reference data, assuming an equal probability for each ensemble member to occur.

Please see https://github.com/matthiasmengel/fast_ant_sid/ for more details on the AIS SID sea level model component calibration and underlying code.

Table S1: Antarctic Ice Sheet (AIS) Solid Ice Discharge (SID) calibration results with optimal parameter sets for the full model ensemble used in DeConto and Pollard [2016]. Optimal values are shown for the calibrated parameters discharge sensitivity α, fast discharge rate γ, reference temperature T_0, and threshold temperature $T_{threshold}$. The Goodness-of-Fit (GOF) is given as RSS weighted by the min/max SLR range for each RCP scenario.

Ensemble member	**α**	γ [mm]	T_0 [°C]	$T_{threshold}$ [°C]	**GOF**
m01	3.65E-05	20.0392	2.1040	2.1862	17.8
m02	8.80E-05	9.2820	1.2398	2.3933	22.27
m03	6.06E-05	7.7926	1.3991	2.2962	24.84
m04	8.62E-05	10.3113	1.2260	2.0377	18.68
m05	6.38E-05	4.5126	2.4634	2.8442	50.13
m06	5.76E-05	7.9647	1.2409	2.2832	23.84
m07	8.04E-05	10.5721	0.9333	2.4897	25.05
m08	5.63E-05	6.4670	2.3359	3.0847	45.24
m09	5.61E-05	7.1438	1.0485	2.4858	22.27
m10	8.10E-05	8.9296	0.8471	2.4802	18.94
m11	5.83E-05	4.5582	2.2093	2.1866	43.96
m12	5.19E-05	7.2404	0.7702	2.1293	18.71
m13	7.77E-05	9.9856	0.7872	2.0468	15.33
m14	4.93E-05	8.4875	2.1888	3.1778	48.7
m15	4.95E-05	7.8439	0.6686	2.2979	18.24
m16	7.36E-05	10.5521	0.5847	2.3745	23.78
m17	4.15E-05	3.3859	0.8490	2.7420	41.36
m18	4.55E-05	7.5651	0.0000	2.9681	42.62
m19	7.25E-05	5.4952	0.0000	1.9160	25.47
m20	3.97E-05	3.0264	0.6514	2.3397	37.86
m21	6.95E-05	7.5224	0.0070	1.8691	25.48
m22	3.90E-05	2.9660	0.5544	2.4036	36.82
m23	3.30E-05	0.0000	0.0000	2.9270	63.06
m24	3.30E-05	0.0000	0.0000	3.1751	86.94
m25	3.88E-05	0.0000	0.0000	3.2424	160.89
m26	4.24E-05	1.6731	0.0574	0.0020	126.29
m27	4.27E-05	2.1206	1.0546	0.0025	29.5
m28	4.13E-05	2.0335	0.9262	0.0016	29.22
m29	4.19E-05	2.0736	0.9770	0.0032	30.02

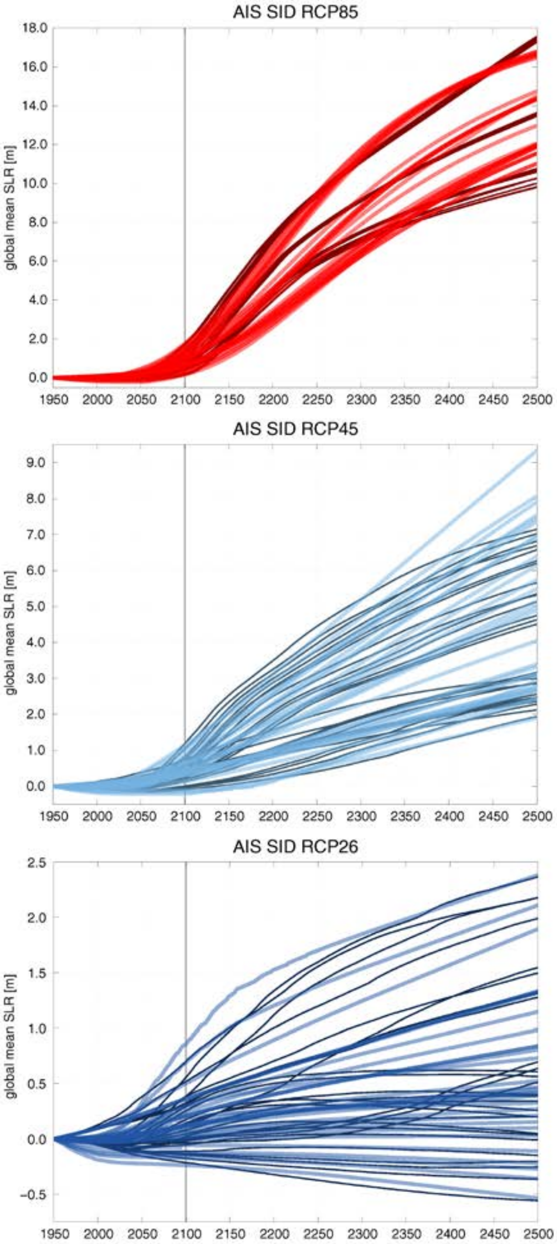

Figure S1: MAGICC AIS SID sea level component calibration results based on the full 29-member model ensemble underlying DeConto and Pollard [2016], forced with RCP 2.6, RCP 4.5, and RCP8.5 CCSM4 temperatures over the calibration period 1950-2500. The panels show scenario-specific calibrated MAGICC global mean SLR responses in metres as colored lines, with underlying reference data as thin dark lines. The 2100 time horizon is indicated by a vertical line.

IPCC AR5 consistent SSP SLR analysis

Table S2: Median estimates and corresponding 66% ranges for global mean SLR projections for quantified SSP scenarios towards the end of the 21st century relative to 1986-2005. The SSPs are pooled according to their radiative Forcing Targets (FTs) and the baseline scenarios without any climate mitigation policies. Absolute SLR estimates are provided in centimeters, the annual rates are given in millimeters per year. Results are based on the Levermann et al. [2014] MAGICC AIS SID sea level component [Nauels et al. 2017].

SSP SLR	FT 2.6	FT 3.4	FT 4.5	FT 6.0	Baselines
2100 [cm rel. to 1986-2005]	51.5 [40.8 to 64.2]	56.6 [44.8 to 70.5]	61.3 [48.4 to 75.9]	67.5 [53.1 to 83.4]	72.4 [56.9 to 90.6]
2081-2100 [cm rel. to 1986-2005]	47.2 [37.6 to 58.5]	51.2 [40.7 to 63.2]	54.8 [43.5 to 67.2]	59.3 [47.1 to 72.6]	62.7 [49.6 to 77.5]
2081-2100 avg. rate [mm/yr]	4.3 [3.3 to 5.9]	5.5 [4.2 to 7.3]	6.6 [5.0 to 8.7]	8.2 [6.2 to 10.7]	9.5 [7.1 to 12.7]

Table S3: 2081-2100 global mean SLR projections for the main sea level components in centimeters relative to 1986-2005, median estimates and corresponding 66% ranges. SMB = Surface Mass Balance. SID = Solid Ice Discharge. The quantified SSP scenarios are pooled according to their radiative Forcing Targets (FTs) and the baseline scenarios without any climate mitigation policies. Results are based on the Levermann et al. [2014] MAGICC AIS SID sea level component [Nauels et al. 2017].

Sea level component	FT 2.6	FT 3.4	FT 4.5	FT 6.0	Baselines
Thermal expansion	18.2 [11.0 to 25.9]	20.6 [12.6 to 28.8]	22.7 [14.1 to 31.3]	25.4 [15.9 to 34.6]	27.3 [17.1 to 37.7]
Glaciers	11.5 [9.5 to 13.8]	12.3 [10.2 to 14.5]	12.9 [10.7 to 15.1]	13.5 [11.3 to 15.7]	14.0 [11.7 to 16.3]
Greenland SMB	2.2 [1.1 to 3.5]	2.5 [1.3 to 4.1]	2.9 [1.6 to 4.6]	3.3 [1.9 to 5.4]	3.8 [2.2 to 6.4]
Greenland SID	3.1 [2.7 to 3.6]	3.2 [2.8 to 3.8]	3.4 [2.9 to 4.1]	3.6 [3.0 to 4.4]	3.8 [3.1 to 4.8]
Antarctic SMB	-1.8 [-2.3 to -1.4]	-2.0 [-2.6 to -1.5]	-2.2 [-2.8 to -1.7]	-2.4 [-3.2 to -1.8]	-2.6 [-3.6 to -1.9]
Antarctic SID	7.0 [3.7 to 12.9]	7.5 [3.9 to 13.9]	7.9 [4.1 to 14.8]	8.5 [4.4 to 15.8]	9.0 [4.6 to 16.8]
Land water storage	5.7 [4.9 to 6.5]	5.7 [4.9 to 6.5]	5.7 [4.9 to 6.5]	5.7 [4.9 to 6.5]	5.7 [4.9 to 6.5]
Total	47.2 [37.6 to 58.5]	51.2 [40.7 to 63.2]	54.8 [43.5 to 67.2]	59.3 [47.1 to 72.6]	62.7 [49.6 to 77.5]

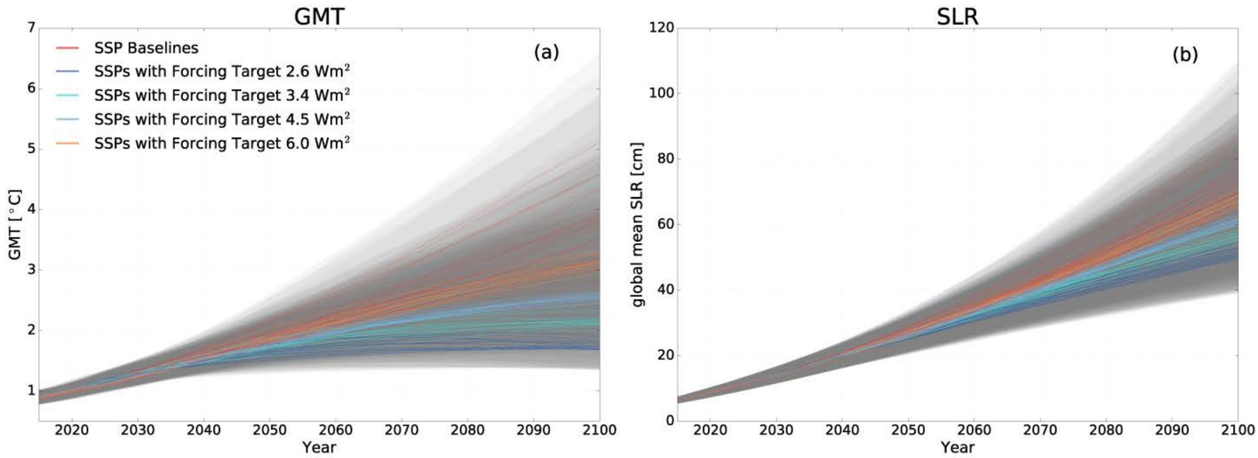

Figure S2: Probabilistic MAGICC GMT (a) and global mean SLR projections (b) with medians and corresponding gray shaded 66% ranges for each member of the SSP scenario ensemble, color coded by specific 2100 radiative forcing targets. Baseline scenario medians are shown in red. GMT anomalies in °C are provided relative to 1850, global mean SLR is given in centimeters relative to the 1986-2005 mean. Results are based on the Levermann et al. [2014] MAGICC AIS SID sea level component [Nauels et al. 2017].

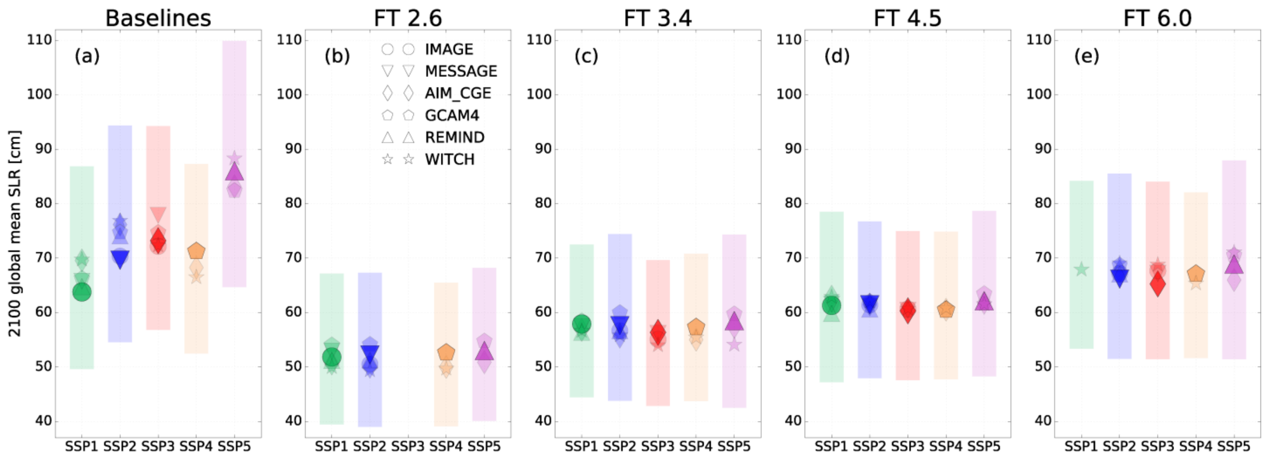

Figure S3: Probabilistic 2100 global mean SLR projections for SPP marker scenarios, showing medians and minimum/maximum 66% ranges for the individual pathways pooled by their radiative Forcing Targets (FTs) and the SSP baseline scenarios. Please note that there are no FT 2.6 realizations available for SSP3, and only one model reaches 6 Wm^{-2} of forcing in 2100 under SSP1 assumptions. Global mean SLR is provided relative to the 1986-2005 mean. Results are based on the Levermann et al. [2014] MAGICC AIS SID sea level component [Nauels et al. 2017].

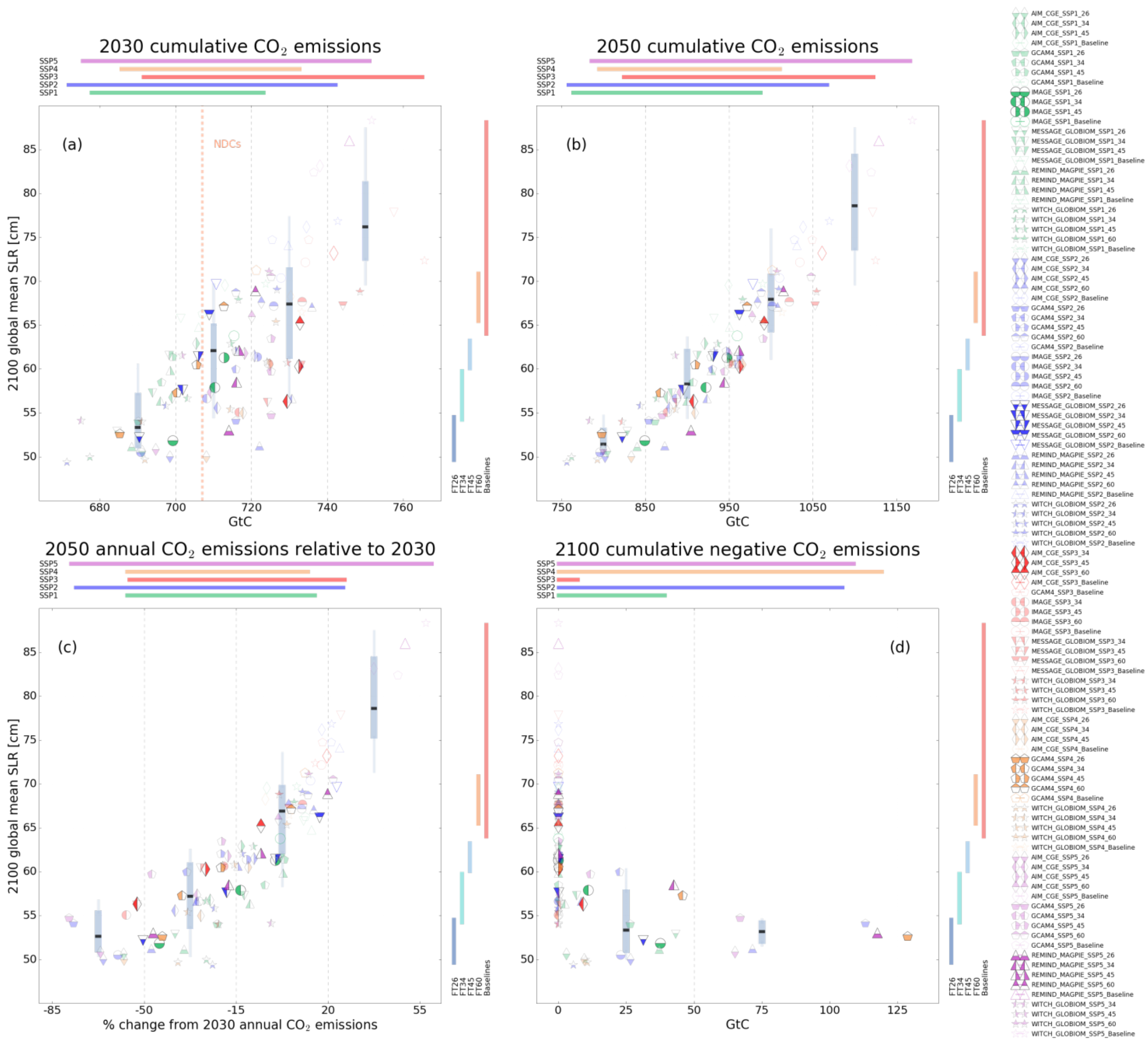

Figure S4: Emission metrics plotted against 2100 global mean SLR medians relative to 1986-2005 for every available SSP scenario. Cumulative CO_2 emissions for 2030 and 2050 in GtC in panels (a) and (b), the relative change in annual CO_2 emissions from 2030 to 2050 in panel (c) and 2100 cumulative net negative CO_2 emissions in panel (d). All CO_2 emissions are shown relative to pre-industrial levels. The SSP scenarios are listed with colors indicating the SSP category and symbols referencing the specific FT. The highlighted pathways represent the marker scenarios for each SSP category. SSP and FT bars on the sides of the panels show corresponding min/max ranges. Vertical boxplots with 90% range whiskers, 50% range boxes and black medians subsume SLR trajectories falling under the individual emission metric categories. The specific categories are shown with dashed vertical gray lines in each panel. The level of cumulative CO_2 emissions currently resulting from the Nationally Determined Contributions (NDCs) [UNFCCC 2016] is shown as dashed orange line in panel (a). Results are based on the Levermann et al. [2014] MAGICC AIS SID sea level component [Nauels et al. 2017].

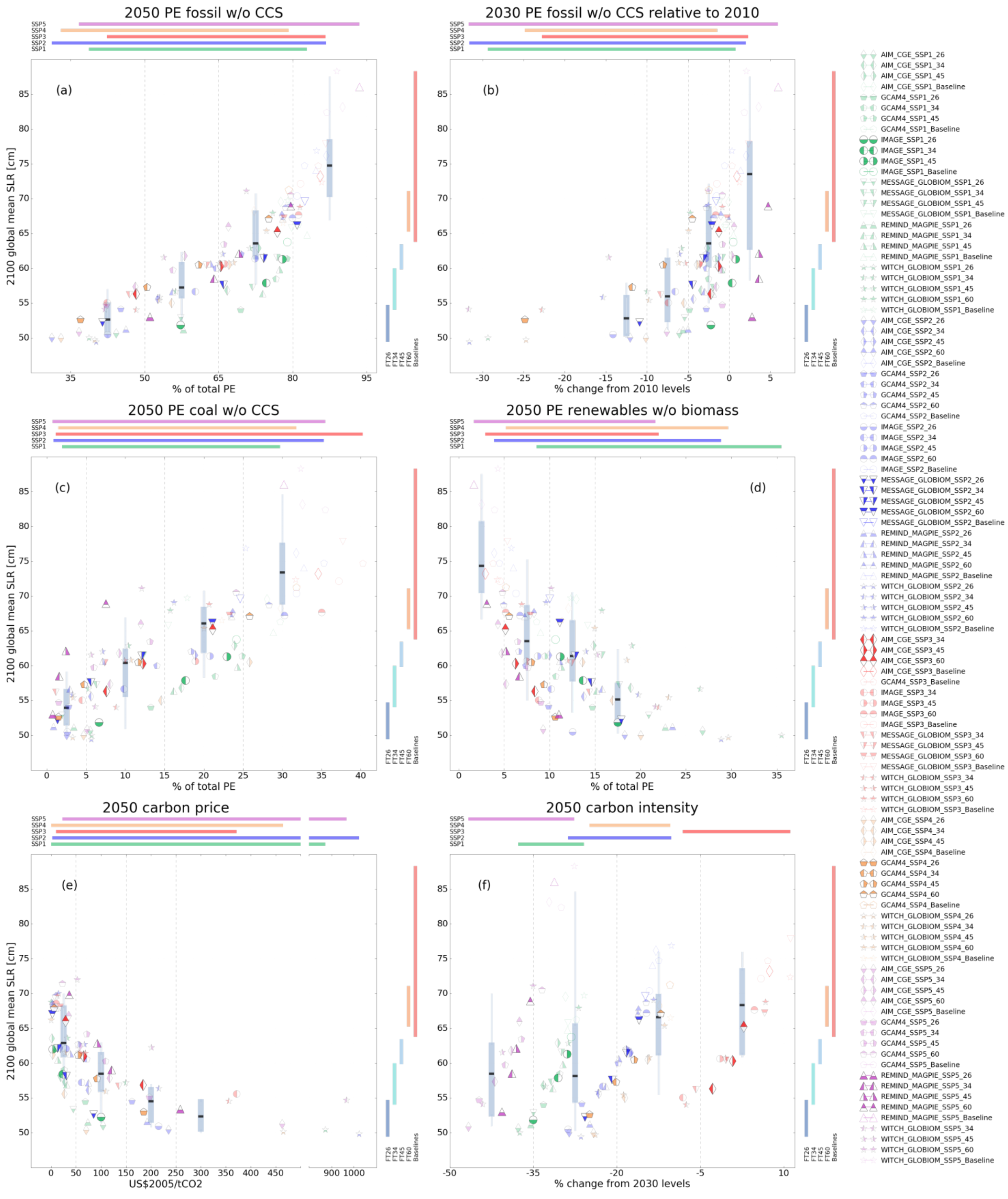

Figure S5: Selected SSP indicators plotted against 2100 global mean SLR medians relative to 1986-2005 for every available SSP scenario. The fractions of 2050 Primary Energy (PE) from non-CCS fossil fuels and 2050 PE from non-biomass renewable energy of 2050 total PE in panels (a) and (c), their relative changes between 2010 and 2030 as percentage from 2010 levels in panels (b) and (d); 2050 carbon price (US$2005 tCO_2^{-1}) in panel (e), percentage change of 2050 carbon intensity relative to 2030 levels in panel (f). PE is expressed using the direct energy equivalence method. The SSP scenarios are listed with colors indicating the SSP category and symbols referencing the specific FT. The highlighted pathways represent the marker scenarios for each SSP category. SSP and FT bars on the sides of the panels show corresponding min/max ranges. Vertical boxplots with 90% range whiskers, 50% range boxes and black medians subsume SLR trajectories falling under the individual emission metric categories. The specific categories are shown with dashed vertical gray lines in each panel. Results are based on the Levermann et al. [2014] MAGICC AIS SID sea level component [Nauels et al. 2017].

References

DeConto, R. M. and Pollard, D. (2016). *Contribution of Antarctica to past and future sea-level rise*, Nature 531 : 591-597.

Flato, G.; Marotzke, J.; Abiodun, B.; Braconnot, P.; Chou, S.; Collins, W.; Cox, P.; Driouech, F.; Emori, S.; Eyring, V.; Forest, C.; Gleckler, P.; Guilyardi, E.; Jakobs, C.; Kattsov, V.; Reason, C. and Rummukainen, M. (2013). *9. Evaluation of Climate Models*. In: Stocker, T. F.; Qin, D.; Plattner, G.-K.; Tignor, M.; Allen, S.; Boschung, J.; Nauels, A.; Xia, Y.; Bex, V. & Midgley, P. M. (Ed.), *Climate Change 2013: The Physical Science Basis. Contribution of Working Group I to the Fifth Assessment Report of the Intergovernmental Panel on Climate Change*, Cambridge University Press, Cambridge, United Kingdom and New York, NY, USA.

Friedlingstein, P.; Andrew, R. M.; Rogelj, J.; Peters, G. P.; Canadell, J. G.; Knutti, R.; Luderer, G.; Raupach, M. R.; Schaeffer, M.; van Vuuren, D. P. and Le Quere, C. (2014). *Persistent growth of CO2 emissions and implications for reaching climate targets*, Nature Geosci 7 : 709-715.

Lagarias, J.; Reeds, J.; Wright, M. and Wright, P. (1998). *Convergence Properties of the Nelder--Mead Simplex Method in Low Dimensions*, SIAM J. Optim. 9 : 112-147.

Levermann, A.; Winkelmann, R.; Nowicki, S.; Fastook, J. L.; Frieler, K.; Greve, R.; Hellmer, H. H.; Martin, M. A.; Meinshausen, M.; Mengel, M.; Payne, A. J.; Pollard, D.; Sato, T.; Timmermann, R.; Wang, W. L. and Bindschadler, R. A. (2014). *Projecting Antarctic ice discharge using response functions from SeaRISE ice-sheet models*, Earth Syst. Dynam. 5 : 271-293.

Meinshausen, M.; Meinshausen, N.; Hare, W.; Raper, S. C. B.; Frieler, K.; Knutti, R.; Frame, D. J. and Allen, M. R. (2009). *Greenhouse-gas emission targets for limiting global warming to 2 degrees C,* Nature 458 : 1158-1162.

Nauels, A.; Meinshausen, M.; Mengel, M.; Lorbacher, K. and Wigley, T. M. L. (2017). *Synthesizing long-term sea level rise projections -- the MAGICC sea level model v2.0*, Geoscientific Model Development 10 : 2495-2524.

Nelder, J. A. and Mead, R. (1965). *A Simplex Method for Function Minimization*, The Computer Journal 7 : 308-313.

Rogelj, J.; Meinshausen, M. and Knutti, R. (2012). *Global warming under old and new scenarios using IPCC climate sensitivity range estimates*, Nature Climate Change 2 : 248-253.

Rogelj, J.; Meinshausen, M.; Sedláček, J. and Knutti, R. (2014). *Implications of potentially lower climate sensitivity on climate projections and policy*, Environmental Research Letters 9 : 031003.